The Roles of Active-Site Residues in the Catalytic Mechanism of *trans*-3-Chloroacrylic Acid Dehalogenase: A Kinetic, NMR, and Mutational Analysis†

Hugo F. Azurmendi,§ Susan C. Wang,‡ Michael A. Massiah,§ Gerrit J. Poelarends,‡ Christian P. Whitman,*,‡ and Albert S. Mildvan*,§

Department of Biological Chemistry, The Johns Hopkins School of Medicine, 725 North Wolfe Street, Baltimore, Maryland 21205-2185, and Division of Medicinal Chemistry, College of Pharmacy, The University of Texas, Austin, Texas 78712-1074

Received November 20, 2003; Revised Manuscript Received January 27, 2004

ABSTRACT: *trans*-3-Chloroacrylic acid dehalogenase (CaaD) converts *trans*-3-chloroacrylic acid to malonate semialdehyde by the addition of H_2O to the C-2, C-3 double bond, followed by the loss of HCl from the C-3 position. Sequence similarity between CaaD, an $(\alpha\beta)_3$ heterohexamer (molecular weight 47 547), and 4-oxalocrotonate tautomerase (4-OT), an $(\alpha)_6$ homohexamer, distinguishes CaaD from those hydrolytic dehalogenases that form alkyl-enzyme intermediates. The recently solved X-ray structure of CaaD demonstrates that βPro-1 (i.e., Pro-1 of the β subunit), αArg-8, αArg-11, and αGlu-52 are at or near the active site, and the $\geq 10^{3,4}$-fold decreases in k_{cat} on mutating these residues implicate them as mechanistically important. The effect of pH on k_{cat}/K_m indicates a catalytic base with a pK_a of 7.6 and an acid with a pK_a of 9.2. NMR titration of ^{15}N-labeled wild-type CaaD yielded pK_a values of 9.3 and 11.1 for the N-terminal prolines, while the fully active but unstable αP1A mutant showed a pK_a of 9.7 (for the βPro-1), implicating βPro-1 as the acid catalyst, which may protonate C-2 of the substrate. These results provide the first evidence for an amino-terminal proline, conserved in all known tautomerase superfamily members, functioning as a general acid, rather than as a general base as in 4-OT. Hence, a reasonable candidate for the general base in CaaD is the active site residue αGlu-52. CaaD has 10 arginine residues, six in the α-subunit (Arg-8, Arg-11, Arg-17, Arg-25, Arg-35, and Arg-43), and four in the β-subunit (Arg-15, Arg-21, Arg-55, and Arg-65). ^{1}H−^{15}N-heteronuclear single quantum coherence (HSQC) spectra of CaaD showed seven to nine Arg-NϵH resonances (denoted R_A to R_I) depending on the protein concentration and pH. One of these signals (R_D) disappeared in the spectrum of the largely inactive αR11A mutant (δH = 7.11 ppm, δN = 89.5 ppm), and another one (R_G) disappeared in the spectrum of the inactive αR8A mutant (δH = 7.48 ppm, δN = 89.6 ppm), thereby assigning these resonances to αArg-11NϵH, and αArg-8NϵH, respectively. ^{1}H−^{15}N-HSQC titration of the enzyme with the substrate analogue 3-chloro-2-butenoic acid (3-CBA), a competitive inhibitor (K_I^{slope} = 0.35 ± 0.06 mM), resulted in progressive downfield shifts of the αArg-8Nϵ resonance yielding a K_D = 0.77 ± 0.44 mM, comparable to the K_I^{slope}, suggestive of active site binding. Increasing the pH of free CaaD to 8.9 at 5 °C resulted in the disappearance of all nine Arg-NϵH resonances due to base-catalyzed NϵH exchange. Saturating the enzyme with 3-CBA (16 mM) induced the reappearance of two NϵH signals, those of αArg-8 and αArg-11, indicating that the binding of the substrate analogue 3-CBA selectively slows the NϵH exchange rates of these two arginine residues. The kinetic and NMR data thus indicate that βPro-1 is the acid catalyst, αGlu-52 is a reasonable candidate for the general base, and αArg-8 and αArg-11 participate in substrate binding and in stabilizing the aci-carboxylate intermediate in a Michael addition mechanism.

The recently discovered haloalkene dehalogenase, *trans*-3-chloroacrylic acid dehalogenase (CaaD)[1], converts the trans isomers of 3-haloacrylates (**1** in Scheme 1) to malonate semialdehyde (**3**), presumably through the unstable halohydrin intermediate **2**, by the addition of water (*1*). The $(\alpha\beta)_3$ heterohexameric CaaD (molecular weight 47 547) is elaborated by the soil bacterium *Pseudomonas pavonaceae* 170 as part of a degradative pathway for *trans*-1,3-dichloropropene, one of the active ingredients in the commercially available fumigants Shell D-D and Telone II (*2*, *3*). Sequence

Scheme 1

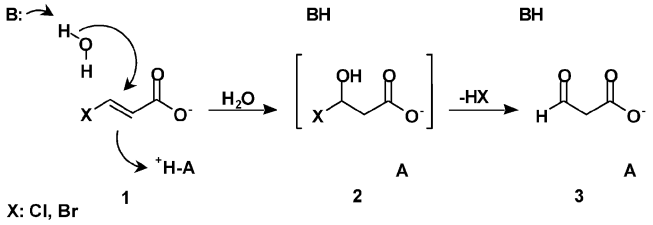

† This research was supported by National Institutes of Health Grants DK-28616 (to A.S.M.) and GM-65324 (to C.P.W.). S.C.W. is a Fellow of the American Foundation for Pharmaceutical Education.

* To whom correspondence should be addressed. A.S.M.: Tel 410-955-2038; fax 410-955-5759; e-mail mildvan@jhmi.edu. C.P.W.: Tel 512-471-6198; fax 512-232-2606; e-mail whitman@mail.utexas.edu.

§ The Johns Hopkins School of Medicine.

‡ The University of Texas.

10.1021/bi030241u CCC: $27.50
Published on Web 03/18/2004

Scheme 2

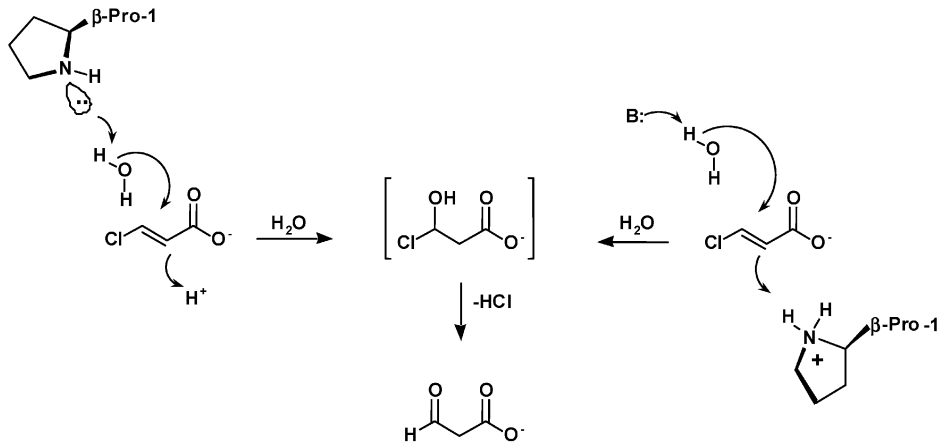

analysis coupled with site-directed mutagenesis placed CaaD in the 4-oxalocrotonate tautomerase (4-OT) family of the tautomerase superfamily and identified Pro-1 of the β-subunit (βPro-1) and Arg-11 of the α-subunit (αArg-11) as mechanistically important residues (*1*). A recent X-ray structure of CaaD placed these residues, as well as αArg-8 and αGlu-52, at or near the active site and confirmed that CaaD is indeed a member of the tautomerase superfamily (*4*).

On the basis of these observations, two different roles may be proposed for the βPro-1 residue (Scheme 2) (*5*). In one mechanism (left), βPro-1 is a *general base*, activating the water for nucleophilic attack at C-3 of **1**. The proton at C-2 comes from solvent or from an unknown acidic residue. In the second mechanism (right), an unknown residue (i.e., B:), possibly αGlu-52, activates the water molecule for attack at C-3, while the proton at C-2 comes from βPro-1, functioning here as a *general acid* catalyst. In the case of 4-OT, Pro-1, with a pK_a of 6.4, has been shown to function as the base catalyst (*6*, *7*), while Arg-11 participates in both substrate binding and catalysis (*8*).

To distinguish between these two roles of Pro-1, we examined the pH dependence of the CaaD-catalyzed reaction, as well as that of the αP1A-CaaD-catalyzed reaction, and independently determined the pK_a values for the amino-terminal prolines in both subunits by direct ^{15}N NMR titration. It has previously been suggested that while both the α- and β-subunits of CaaD have an amino-terminal proline, only the βPro-1 was required for activity (*1*). The results of our studies indicate that βPro-1 functions as the general acid catalyst, identifying a new role for the conserved catalytic amino-terminal proline in the tautomerase superfamily. In addition, we examined the roles of arginines and provide direct evidence for the participation of αArg-8 and αArg-11 in catalysis. On the basis of these results, a catalytic mechanism for the CaaD-catalyzed reaction is proposed. A preliminary abstract of this work has been published (*5*).

[1] Abbreviations: Ap, ampicillin; BAA, *trans*-3-bromoacrylic acid; CAA, *trans*-3-chloroacrylic acid; CaaD, *trans*-3-chloroacrylic acid dehalogenase; 3-CBA, 3-chloro-2-butenoic acid; ESI-MS, electrospray ionization mass spectrometry; HPLC, high-pressure liquid chromatography; HSQC, heteronuclear single quantum coherence; IPTG, isopropyl-β-D-thiogalactoside; Kn, kanamycin; LB, Luria−Bertani medium; 4-OT, 4-oxalocrotonate tautomerase; PCR, polymerase chain reaction; SDS−PAGE, sodium dodecyl sulfate−polyacrylamide gel electrophoresis.

EXPERIMENTAL PROCEDURES

Materials. The *trans*-3-chloroacrylic acid was obtained from Fluka Chemical Corp. (Milwaukee, WI), and the *trans*-3-bromoacrylic acid was synthesized as described (*9*). Tryptone, yeast extract, and agar were obtained from Becton, Dickinson, and Company (Franklin Lakes, NJ). The Ultrafree DA centrifugal filter units, the YM-3 ultrafiltration membranes, and the Amicon concentrators were obtained from Millipore Corp. (Bedford, MA). The thin-walled PCR tubes were obtained from Ambion, Inc. (Austin, TX). Restriction enzymes, PCR reagents, and T4 DNA ligase were obtained from F. Hoffman-LaRoche, Ltd. (Basel, Switzerland), Promega Corp. (Madison, WI), or New England Biolabs (Beverly, MA). The Wizard PCR Preps DNA purification systems were purchased from Promega Corp. The QIAprep Spin Miniprep kit was obtained from Qiagen Inc. (Valencia, CA). Other molecular biology reagents, including agarose, DNA ladders, and protein molecular standards, were obtained from Invitrogen Corp. (Carlsbad, CA). Oligonucleotides for DNA amplification and sequencing were synthesized by either Oligos Etc. (Willsonville, OR) or Genosys (The Woodlands, TX). The remaining reagents, buffers, and solvents were obtained from Sigma Aldrich Chemical Co. (St. Louis, MO), Fisher Scientific Inc. (Pittsburgh, PA), Spectrum Laboratory Products, Inc. (New Brunswick, NJ), or EM Science (Cincinnati, OH). The construction of the βP1A, αR11A, αR8A, and αE52Q mutants has been described elsewhere (*4*, *9*).

Strains and Plasmids. Escherichia coli strains DH5α (Invitrogen) and JM109 (Promega) were used for cloning and isolation of plasmids. *E. coli* strains BL21(DE3)pLysS from Novagen and BL21-Gold(DE3)pLysS from Stratagene (La Jolla, CA) were used for recombinant protein expression.

General Methods. Techniques for restriction enzyme digestions, ligation, transformation, and other standard molecular biology manipulations were based on methods described elsewhere (*10*) or as suggested by the manufacturer. Plasmid DNA was introduced into cells by electroporation using a Cell-Porator Electroporation System (Whatman Biometra, Göttingen, Germany). The PCR was performed in a DNA thermal cycler (model 480) obtained from PerkinElmer Inc. (Wellesley, MA). DNA sequencing was done at the DNA Core Facility in the Institute for Cellular and Molecular Biology at the University of Texas (Austin).

Kinetic data were obtained on an Agilent 8453 diode array spectrophotometer. The cuvettes were mixed using a stir/add cuvette mixer (Bel-Art Products, Pequannock, NJ). The kinetic data were fitted by nonlinear regression data analysis using the Grafit program (Erithacus Software Ltd., Horley, U.K.) obtained from Sigma Chemical Co. HPLC was performed on a Waters (Milford, MA) 501/510 system or a Beckman System Gold HPLC (Fullerton, CA) using a TSKgel Phenyl-5PW hydrophobic column (TosoHaas, Montgomeryville, PA) or a Superose 12 gel filtration column (Amersham Biosciences, Piscataway, NJ). Protein was analyzed by Tris glycine sodium dodecyl sulfate−polyacrylamide gel electrophoresis (SDS−PAGE) under denaturing conditions on 17.5% gels using either the Mini-Protean II or Mini-Protean III vertical gel electrophoresis apparatus obtained from Bio-Rad (Hercules, CA) (*11*). Protein concentrations were determined from the difference in absorbances at 215 and 225 nm which, when multiplied by the factor 144, gives the concentration in micrograms per milliliter (*12*).

Site-Directed Mutagenesis. The αP1A CaaD mutant was constructed using the gene for the α-subunit of CaaD [in pET-24a(+)] as the template (*9*). The gene is flanked by an *Nde*I restriction site and a *Not*I restriction site. The mutation was introduced by overlap extension PCR (*13*). The external PCR primers were oligonucleotides 5′-GCGGATAACAATTCCCCTCT-3′ (designated primer A) and 5′-CTCAGCTTCCTTTCGGGCTT-3′ (designated primer D). Primer A corresponds to a region 36 bases upstream of the *Nde*I restriction site in the pET-24a(+) vector. Primer D corresponds to the complementary sequence of a region 20 bases downstream of the His-tag region in both pET-21a(+) and pET-24a(+). The internal primers were 5′-AGAGATCAT*CGC*CATATGTATATC-3′ (primer B) and 5′-GATATACATATG*GCG*ATGATCTCT-3′ (primer C). In each internal primer, the codon for the desired mutation is italic and the remaining bases correspond to the coding (primer C) or the complementary sequence (primer B). The AB, CD, and AD fragments were constructed and purified as described elsewhere (*9*). Restriction digests of the pET-24a(+) vector and the AD fragment were performed at 37 °C for 6 h followed by purification using gel electrophoresis and the Ultrafree-DA units. The ligation reaction was performed using the Quick Ligation Kit (New England Biolabs, Inc., Beverly, MA). The ligated plasmids were purified by ethanol precipitation and resuspended in sterile water (5 μL). The purified DNA (2 μL) was used to transform *E. coli* DH5α by electroporation. Transformed cells were plated onto LB/Kn (50 μg/mL) plates for selection. Two colonies were selected at random for insert sequencing. One of the isolated plasmids, designated pET-24a(+)-CaaD-αP1A-1, had only the desired mutation in the insert.

Overexpression and Purification of the αP1A-CaaD Mutant. For expression, pET-24a(+)-CaaD-αP1A-1 was cotransformed into *E. coli* strain BL21-Gold(DE3)pLysS by electroporation, along with pET-21a-CaaDβ4 (containing the gene for the β-subunit of CaaD). Cells were selected in triple antibiotic media as described (*9*), and subsequent growth and purification were performed as described for wild-type CaaD (*9*). Typically, a 3L culture of the αP1A-CaaD mutant yields 9 g of cells and 25 mg of protein, which was >95% homogeneous as assessed by SDS−PAGE. The subunit masses of the α-P1A-CaaD mutant were determined using an LCQ electrospray ion trap mass spectrometer (ThermoFinnigan, San Jose, CA), housed in the Analytical Instrumentation Facility Core in the College of Pharmacy at the University of Texas at Austin. The sample was prepared as described elsewhere (*9*). The observed monomer masses for the α- and β-subunits of αP1A-CaaD, as found by electrospray mass spectroscopy, were 8315.9 (calcd 8318.0) and 7505.3 (calcd 7507.0), respectively.

^{15}N Labeling of Wild-Type CaaD and CaaD Mutants. For the NMR studies, the wild-type and the αP1A and αR11A mutant enzymes were ^{15}N-labeled by a modification of literature protocols described below, while the αR8A mutant was labeled as previously described (*6*). The M9 minimal medium (*10*, *14*) was enriched with supplements found in the MOPS minimal media (*15*) and $^{15}NH_4Cl$ (99% enriched). All other nitrogen sources (e.g., nitrates, unlabeled NH_4Cl) were removed. Accordingly, in 1 L of culture medium were 5 × M9 salts containing a 25% (w/v) solution of $^{15}NH_4Cl$ (2 mL), 1 M $MgSO_4$ (2 mL), 20% glucose (20 mL), 1 M $CaCl_2$ (100 μL), 1 mg/ml thiamine solution (1.14 mL), vitamin supplement solution (*6*, *15*) (1.14 mL), 5 mg/mL thymine−uracil solution (1.4 μL), and Mg^{2+} micronutrient solution (1 mL) (*6*, *15*).

Cultures of LB media (25 mL) containing both ampicillin (100 μg/mL) and kanamycin (50 μg/mL) were inoculated from single colonies of the expression strain for the appropriate enzyme (wild-type, αP1A, and αR11A) and grown overnight at 37 °C. Subsequently, cultures (500 mL) of the M9 medium described above and Ap/Kn (100 and 50 μg/mL, respectively) were inoculated with 3 mL of the overnight culture and incubated at 30 °C with vigorous shaking. When the OD_{600} reading reached ∼0.8, the cultures were induced with IPTG (1 mM) and then allowed to continue to grow at 30 °C. Additional aliquots of ampicillin (50 μg/mL) and kanamycin (25 μg/mL) were added to each culture to assist in plasmid retention. After a 24 h total growth period, cells were harvested by centrifugation and stored at −80 °C until use.

Typically, 5 L of culture yields 30 g of cells for CaaD, 25 g for the αP1A mutant, and 30 g for the αR11A and αR8A mutants. Due to low yields of enzyme, 10−20 L of culture were processed in each purification procedure, which was performed as described previously (*9*). If the protein contained contaminants after the G-200 column, the concentrated protein was made 1 M in ammonium sulfate and reloaded onto the phenyl-5PW column for final purification. Typically, the yields per liter of culture are as follows: CaaD, 1−3 mg; the αP1A mutant, 35 mg; the αR11A mutant, 27 mg; the αR8A, 5 mg. We have not determined the reason for the low yields of wild-type CaaD in minimal media.

Enzymatic Assay. Kinetic assays were performed in 20 mM Na_2HPO_4 buffer, pH 9.0, observing the decrease in absorbance at 224 nm corresponding to the hydration of *trans*-3-chloroacrylate or *trans*-3-bromoacrylate as described (*9*). An aliquot of CaaD, either wild-type or mutant, was diluted into buffer within a cuvette and assayed by the addition of a small quantity of a substrate stock solution to cover a concentration range between 10 and 150 μM. A 50 mM stock solution was prepared by dissolving the appropriate amount of substrate in 100 mM Na_2HPO_4 buffer, pH 9.2, resulting in a final pH of ∼7.3.

Inhibition Studies. To synthesize 3-chloro-2-butenoic acid (3-CBA), the commercially available 2-butynoic acid (1 g, 11.9 mmol) was dissolved in concentrated HCl (10 mL) and heated at 80 °C for 1.5 h. After cooling to room temperature, the mixture was extracted with ethyl acetate (3 × 10 mL). The ethyl acetate layers were combined, dried over anhydrous $MgSO_4$, and evaporated to dryness. Crystallization from hexanes/CH_2Cl_2 afforded 0.54 g (38% yield) of the inhibitor as a 6:1 (*Z*/*E*) mixture as determined by ^{1}H NMR analysis. *Z*-isomer: ^{1}H NMR ($CDCl_3$, 250 MHz on a Bruker AM 250 spectrometer) δ 2.28 (3H, d), 6.05 (1H, q); ^{13}C NMR (CD_3-OD, 62 MHz) δ 28.0 (s, C4), 118.0 (s, C2), 146.9 (s, C1). *E*-isomer: ^{1}H NMR ($CDCl_3$, 250 MHz) δ 2.58 (3H, d), 6.09 (1H, q); ^{13}C NMR (CD_3OD, 62 MHz) δ 23.5 (s, C4), 120.5 (s, C2), 167.0 (s, C1). 3-Chloro-2-butenoic acid (as a 6:1 *Z*/*E* mixture) was made as a 6.7 mg/mL solution in 100 mM Na_2HPO_4 buffer, resulting in a 54.8 mM stock solution at pH 7.0. A quantity of CaaD (160 μL of an 11.0 mg/mL solution in 20 mM NaH_2PO_4 buffer, pH 7.3) was equilibrated in 20 mM NaH_2PO_4 buffer, pH 9.0 (80 mL), for at least an hour at room temperature. Subsequently, this enzyme solution was divided into 14 mL portions. The inhibitor was added to the desired final approximate concentration (0−384 μM) and allowed to equilibrate for ~5 min. Aliquots (1 mL) were withdrawn and assayed for activity using 12 concentrations of BAA as the substrate (10−150 μM).

pH Dependence of Kinetic Parameters of CaaD Using BAA. The dependence of the rate of hydration of *trans*-3-bromoacrylic acid was determined in 20 mM sodium phosphate buffer, pH range 6.5−10.3. *trans*-3-Bromoacrylic acid, BAA, rather than CAA was used as the substrate because of its higher extinction coefficient. The buffers were made up by combining appropriate quantities of 20 mM NaH_2PO_4, 20 mM Na_2HPO_4, and 20 mM Na_3PO_4 buffers to maintain constant ionic strength. For each pH value, a sufficient quantity of enzyme (from a stock solution of 8.5 mg/mL in 20 mM NaH_2PO_4, pH 7.3) was equilibrated in buffer (40 mL) for ≥1 h at 29 °C. The addition of the large amount of enzyme changed the pH, so the reported pH values (6.50−10.26) are those determined after the addition of the enzyme. Subsequently, aliquots (1 mL) were removed and assayed for activity using 12 BAA concentrations ranging from 10 to 150 μM from stock solutions of substrate that were made up as described (*9*). The volume of substrate added was 8 μL or less in all experiments. More accurate *initial rates* were obtained by varying the enzyme concentration rather than the incubation time. The volumes of stock enzyme solution added were 8 μL/mL (pH 6.5), 5 μL/mL (pH 7.0−7.4), 4 μL/mL (pH 8.0−8.9), 4.5 μL/mL (pH 9.0), 6 μL/mL (pH 9.4−9.8), 9 μL/mL (pH 10.0), and 10 μL/mL buffer (pH 10.3). To show that the reduced activity at high pH was due to the enzymatic reaction (and not the result of irreversible denaturation), CaaD (20 μL) was equilibrated at room temperature in the phosphate buffer (2 mL, pH 10.5) for 2 h. An aliquot (200 μL) was subsequently diluted into phosphate buffer (pH 9.0) and immediately assayed at two concentrations of BAA (100 and 150 μM). The resulting activity was comparable to that expected for the wild-type enzyme at pH 9.0, indicating that CaaD was not irreversibly denatured at the high pH values investigated.

The pH rate profile for the α-P1A mutant of CaaD was determined using a procedure similar to that described above at 22 °C. The range of final pHs was 6.5−10.8. The amounts of enzyme (18.0 mg/mL stock in 20 mM NaH_2PO_4, pH 7.3) used were 1.5 μL/mL of buffer (pHs 6.5 and 10.8), 1 μL/mL of buffer (pH 7.0 and 9.5), 0.75 μL/mL of buffer (pH 7.5−9.3), and 2.5 μL/mL of buffer (pH 10.3).

NMR Spectroscopy. All NMR data on the proteins were collected on a Varian INOVA 600 MHz spectrometer equipped with a pulse field gradient unit, using Varian probes, either a 5 mm triple resonance actively shielded *z*-gradient probe for HSQC spectra or a 5 mm broadband probe for ^{15}N 1D NMR spectroscopy. The pK_a of the amino groups of the two N-terminal prolines were determined by monitoring the pH dependence of the ^{15}N-chemical shift of the secondary amino nitrogen resonance (*7*). The ^{15}N chemical shifts were referenced to external liquid ammonia as described (*16*). Spectra were acquired without proton decoupling. The titrations were performed using ^{15}N-labeled samples with concentrations as indicated, at 22 °C, by adding small aliquots (typically 1 μL) of 1 M HCl or NaOH to the samples. The acquisition parameters were as follows: spectral width, 14 000 Hz; acquisition time, 0.512 s; relaxation delay, 0.6 s; total number of transients, 4000−75 000. The spectra were processed with the program NMRPipe (*17*) using line broadenings of 10−80 Hz and zero-filling to 16 000 points. Chemical shifts were determined by placing the cursor on the resonance peak of expanded spectra. Within error (<0.1 ppm), the peak detecting module of NMRPipe gave the same chemical shifts. The titration of wild-type CaaD was found to be reversible by ^{1}H−^{15}N-HSQC criteria, except for a small amount of precipitation produced in the process. In contrast, the αP1A mutant was much more sensitive to prolonged incubation and to extremes of pH outside the range of 6−9.5, resulting in progressive decreases in signal intensity during the titration. The pK_a values were determined from nonlinear least-squares fit of the data to eq 1, where n is the Hill coefficient and δ_1 and δ_2 are the limiting chemical shifts at low and high pH, respectively (*7*).

$$\delta\ (\text{ppm}) = \frac{\delta_1 + \delta_2(10^{\text{pH}-\text{p}K_a})^n}{(10^{\text{pH}-\text{p}K_a})^n + 1} \qquad (1)$$

Selective ^{1}H−^{15}N-HSQC spectra of the arginine NϵH region (*8*, *18*) were acquired from uniformly ^{15}N-labeled samples of wild-type CaaD and the αR8A and αR11A mutants in sodium phosphate buffer solutions under the conditions of temperature, pH, and concentration indicated in the figure legends. The wild-type sample was also used for NMR titrations with the substrate analogue, 3-chlorobutenoic acid (3-CBA), as the 6:1 *Z*/*E* isomeric mixture. The parameters used were as follows: spectral widths of 1000 and 5000 Hz for ^{15}N and ^{1}H, respectively, with 128 and 1024 complex points in the indirect and direct dimensions, respectively; acquisition time in the direct dimension, 0.1024 s; relaxation delay, 1.0 s. The dissociation constant (K_D) of 3-CBA was obtained from the effects of its concentration on the chemical shift changes ($\Delta\delta_{obs} = |\delta - \delta_0|$, where δ_0 is the initial chemical shift) of the assigned

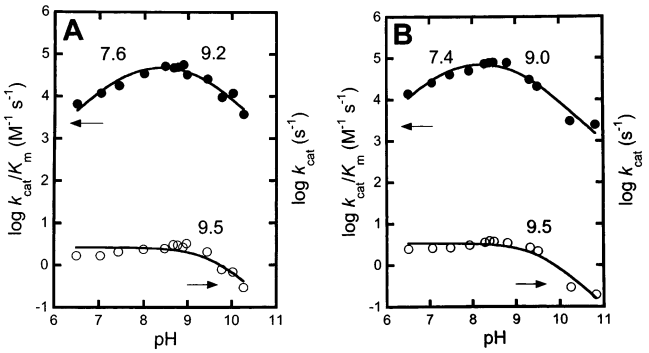

FIGURE 1: pH dependence of the kinetic parameters for the dehalogenation of *trans*-3-bromoacrylate catalyzed by CaaD. The pH dependence of log(k_{cat}/K_m) (●) and log k_{cat} (○) is shown for (A) wild-type CaaD and (B) the αP1A mutant. The curves were computed from nonlinear least-squares fitting of the data to eqs 3 and 4, respectively, yielding the parameters given in the text. Components and conditions were 20 mM NaH_2PO_4 buffer, $T = 29$ (A) and 22 °C (B).

Table 1: Kinetic Parameters for the Dehalogenation of CAA and BAA by Wild-Type CaaD and Mutants[a]

enzyme	substrate	k_{cat} (s^{-1})	K_m (μM)	k_{cat}/K_m (M^{-1} s^{-1})
wild type[b]	CAA	3.8 ± 0.1	31 ± 2	$(1.2 \pm 0.1) \times 10^5$
	BAA	5.1 ± 0.1	37 ± 2	$(1.4 \pm 0.1) \times 10^5$
αP1A	CAA	2.5 ± 0.1	33 ± 2	$(7.4 \pm 0.7) \times 10^4$
	BAA	3.9 ± 0.1	43 ± 3	$(9.1 \pm 0.9) \times 10^4$
βP1A[c]	CAA	$<1.5 \times 10^{-3}$		
αR8A[c,d]	CAA	$<1.5 \times 10^{-3}$		
αR11A[c]	CAA	$(1.5 \pm 0.2) \times 10^{-3}$		
αE52Q[d]	CAA	$<1.5 \times 10^{-3}$		

[a] Determined in 20 mM sodium phosphate buffer, pH 9.0, at 23 °C. [b] From ref *9*. [c] Calculated from the error levels reported in ref *9*. [d] From refs *4* and *5*.

resonance of αArg8-Nϵ by fitting the data to eq 2, as described (*8*).

$$\Delta\delta_{obs} = \Delta\delta_{max}[(K_D + L_{tot} + E_{tot}) - \sqrt{(K_D + L_{tot} + E_{tot})^2 - 4L_{tot}E_{tot}}]/(2E_{tot}) \quad (2)$$

In eq 2, L_{tot} is the total ligand concentration and E_{tot} is the total enzyme active site concentration.

RESULTS AND DISCUSSION

Effect of pH on k_{cat}/K_m of CaaD. To distinguish between the two potential roles of βPro-1 in the mechanism of CaaD (Scheme 2), we determined the pK_a values of potential acid and base catalysts by pH rate studies. The pH dependences of the steady-state kinetic parameters for the CaaD-catalyzed hydration of *trans*-3-bromoacrylate (**1**, BAA) were determined in 20 mM sodium phosphate buffer over the pH range 6.5−10.5 at 29 °C. The low values of k_{cat}/K_m and of k_{cat} for BAA at pH 9.0 (1.4×10^5 M^{-1} s^{-1} and 5.1 ± 0.1 s^{-1}, respectively) (Table 1) suggest that the enzyme−substrate complex is in rapid equilibrium with the free enzyme and free substrate so that the pH dependences of k_{cat}/K_m and of k_{cat} can be analyzed with eq 3 using rapid equilibrium assumptions (*7*, *19*). Very similar kinetic parameters have been found with *trans*-3-chloroacrylic acid (CAA) (Table 1).

$$\frac{k_{cat}}{K_m} = \frac{(k_{cat}/K_m)^{max}}{1 + \frac{[H^+]}{K_{H2E}} + \frac{K_{HE}}{[H^+]}} \quad (3)$$

In eq 3, K_{H2E} and K_{HE} are the dissociation constants of the basic and acidic groups respectively, in the free enzyme, which are important for catalysis. A plot of log k_{cat}/K_m versus pH shows a bell-shaped dependence with slopes of +1 and −1 on the ascending and descending limbs, respectively (Figure 1A), consistent with eq 3, indicating that both a basic group (ascending limb) and acidic group (descending limb) are important for catalysis. The substrate (p$K_a = 4.6$) does not titrate in the pH range studied. A nonlinear least-squares fit of these data to eq 3 gave pK_a values of 7.6 ± 0.2 and 9.2 ± 0.2, respectively, for these groups in the free enzyme.

Kinetic Parameters of the αP1A Mutant of CaaD. While both the α- and β-subunits of CaaD have an amino-terminal proline, the results of mutagenesis suggested that only the βPro-1 residue participates in catalysis (*1*). However, the activity of the αP1A mutant was previously measured in cell extracts by a colorimetric assay, which did not enable accurate measurements of kinetic parameters (*1*). In view of these observations, the αP1A mutant was constructed by overlap PCR, the mutant protein purified, and its kinetic parameters determined using the more sensitive kinetic assay described in ref *9*. The values of k_{cat}, K_m, and k_{cat}/K_m obtained for the hydration of BAA catalyzed by the αP1A mutant of CaaD are very similar to those found with the wild-type enzyme (Table 1). It was also determined that the αP1A mutant processed 2-oxo-3-pentynoate to acetopyruvate (data not shown) with kinetic parameters comparable to those of the wild-type enzyme (*9*), thereby providing further evidence that the αP1A mutant carries out a hydration reaction. These observations confirm that only the βPro-1 residue is involved in catalysis.

The pH dependences of the steady-state kinetic parameters in the αP1A-CaaD-catalyzed hydration of BAA were also determined over the pH range 6.5−10.8 at 22 °C. The log k_{cat}/K_m vs pH profile is also bell-shaped with slopes of unity and pK_a values of 7.4 ± 0.2 and 9.0 ± 0.2 in the free enzyme (Figure 1B), very similar to those obtained with the wild-type enzyme.

Effect of pH on k_{cat} of CaaD and of the αP1A Mutant. At saturating levels of the substrate BAA, with both the wild-type enzyme and the αP1A mutant, the pH dependences of k_{cat} show the pK_a of the basic group to become undetectable (Figure 1A,B), suggesting that it has decreased to a value below 6.0. This behavior can be fit by eq 4, in which K_{H2ES} and K_{HES} are the dissociation constants of the basic and acidic groups, respectively, in the enzyme−substrate complex, which are important in catalysis.

$$k_{cat} = \frac{(k_{cat})^{max}}{1 + \frac{[H^+]}{K_{H2ES}} + \frac{K_{HES}}{[H^+]}} \quad (4)$$

In the present case $K_{H2ES} \gg [H^+]$ causing the middle term in the denominator to disappear. The pK_a of the acidic group has increased to 9.5 ± 0.1 in the BAA complex (Figure 1), possibly as a result of the nearby carboxylate group of the

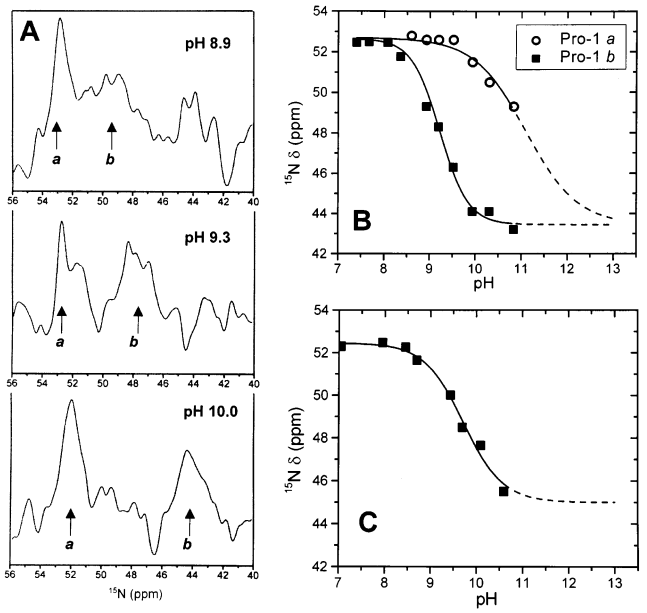

FIGURE 2: Determination of the pK_a of the amino terminal prolines by ^{15}N NMR spectroscopy as a function of pH. Panel A shows typical ^{15}N NMR spectra showing the pH dependence of the chemical shifts of Pro-1 ^{15}N resonances. Signals marked a and b were assigned to αPro-1N and *β*Pro-1N, respectively, as described in the text. Panel B shows the pH titration curves for the amino nitrogen atoms of αPro-1 (○) and *β*Pro-1 (■) in wild-type CaaD. The pK_a values, from nonlinear least-squares fitting to eq 1, are 11.1 ± 0.2 and 9.3 ± 0.1 for αPro-1 and *β*Pro-1, respectively. Panel C shows the pH titration curve for the amino nitrogen atom of *β*Pro-1 in the αP1A mutant fitted to eq 1 with a pK_a of 9.7 ± 0.3. Components and conditions were 1.5 mM in CaaD active sites, 8 mM NaH_2PO_4 buffer, and 10% D_2O at 22 °C. The spectra were processed using 30 Hz line broadening.

bound substrate. Extension of these studies beyond the pH range of 6−11 is precluded by enzyme denaturation.

Determination of the pK_a Values of the N-Terminal Prolines by Direct ^{15}N NMR Titration. To assign the kinetically determined pK_a values, pH titrations of the uniformly ^{15}N-labeled wild-type CaaD were carried out using ^{15}N NMR spectroscopy (*7*). Although we have previously shown that the ^{15}N-chemical shifts of Pro-1 in 4-OT and in several mutants are well resolved (*7*, *20*), titration of CaaD is complicated by the fact that both the α- and *β*-subunits have an amino-terminal proline, only one of which (*β*Pro-1) functions in catalysis (*1*) (Table 1). Accordingly, at pH 8.9, the ^{15}N NMR spectrum of CaaD shows two Pro-1 ^{15}N resonances (Figure 2A), an upfield signal at 49.3 ppm (signal b) and a downfield signal at 52.6 ppm (signal a). The chemical shifts of these ^{15}N resonances were followed over the pH range 6.5−10.8 (Figure 2A,B). The resulting titration curves yield a pK_a of 9.3 ± 0.1 and a Hill coefficient of 0.9 ± 0.2 for the upfield signal and a pK_a of 11.1 ± 0.2 and a Hill coefficient of 0.7 ± 0.3 for the downfield signal (assuming the same end points as found for the upfield signal, Figure 2B). These titrations suggest that at pH values ≥8, the upfield signal (signal b) corresponds to *β*Pro-1 and the downfield signal (signal a) corresponds to αPro-1.

These assignments were tested by ^{15}N NMR titrations of the fully active αP1A mutant (Table 1), which showed only a single Pro-1 resonance at pH 8.9, yielding a pK_a of 9.7 ± 0.3, and a Hill coefficient of 1.0 ± 0.2 (Figure 2C). The overlap of this pK_a with that observed for the upfield proline resonance in wild-type CaaD confirms that Pro-1 of the *β* subunit (*β*Pro-1) is the general acid catalyst, which protonates C-2 of BAA in the mechanism of CaaD. The slightly higher pK_a value of 9.7 ± 0.3 found with two preparations of the αP1A mutant is probably related to its instability at pH values ≥9.5, resulting in line broadening, which increased the errors in the chemical shift measurements. ^{1}H−^{15}N-HSQC spectra of the αP1A mutant acquired before and after the pH titrations and activity assays also showed evidence of partial denaturation at high pH, not observed with the wild-type enzyme. Nevertheless, the results with the αP1A mutant confirm the assignments of the resonance with a pK_a of 9.3 as that of *β*Pro-1 and the resonance with a pK_a of 11.1 as that of αPro-1. Hence *β*Pro-1 has the appropriate pK_a to function as the acid catalyst in CaaD.

Comparison of the Roles of Pro-1 in CaaD and 4-OT. Tautomerase superfamily members are structurally homologous proteins, which share a common *β*-α-*β* structural fold (*21*−*23*), as well as a catalytic Pro-1 (*6*, *7*). In the bacterial isomerase 4-OT, the best-characterized member of this superfamily, Pro-1 functions as a general base in the reaction, which transforms *β*,*γ*-unsaturated enones to their α,*β*-isomers via a dienol intermediate (*6*, *7*). In 4-OT, Pro-1 can function effectively as a general base at cellular pH because it has a pK_a of 6.4, as determined by a pH rate profile and by direct ^{15}N NMR titration (*6*, *7*). This pK_a is 3 pH units lower than that observed for the model compound, proline amide (pK_a = 9.4) (*7*), as a result of the presence of Pro-1 in a hydrophobic active site with a local effective dielectric constant of approximately 14 (*20*). The fact that Pro-1 has been implicated as the catalytic *base* in all superfamily members characterized to date suggested that Pro-1 might behave similarly in other superfamily members, such as CaaD. However, the present results indicate that *β*Pro-1 functions as general *acid* catalyst in CaaD, thereby defining a new role for the conserved catalytic amino-terminal proline in the tautomerase superfamily. In view of the fact that CaaD carries out a hydration reaction, it is not unexpected that the active site would be more hydrophilic than that of 4-OT so that *β*Pro-1 would have the high pK_a value predicted for an exposed amino-terminal group.

Base Catalysis in CaaD. From the ascending limb of the pH versus k_{cat}/K_m profile of CaaD, a residue with a pK_a of 7.6 ± 0.2 in the free enzyme, which must be deprotonated for activity, may be the general base catalyst involved in the activation of water (Figure 1). The pH versus k_{cat} rate profile lacks an ascending limb, suggesting that this pK_a may have decreased to a value below 6.0 in the enzyme−substrate complex. Of the residues known to contribute significantly to catalysis (Table 1), αGlu-52 is a reasonable candidate, although a pK_a of 7.6 is too high by ∼3 pH units for an exposed glutamate residue. Hence αGlu-52 may be buried in a hydrophobic environment in the free enzyme. In the enzyme−substrate complex, αGlu-52 must become exposed to water to activate it, which would lower the pK_a of αGlu-52 to ∼5.0, as suggested by the loss of the ascending limb in the pH versus k_{cat} profile (Figure 1A,B). It was, however, not possible to measure k_{cat} below pH 6 because of enzyme denaturation. In the 2.3 Å X-ray structure of affinity-labeled CaaD (*4*), a carboxylate oxygen of αGlu-52 is 2.5 Å from a water and 5.1 Å from the nitrogen of *β*Pro-1. No other glutamate, aspartate, or histidine residues are within 10 Å

Table 2: ^{15}N and ^{1}H Chemical Shift Values in ppm for the Side Chain ^{15}Nϵ Nitrogen and NϵH Proton Resonances of the Detectable Arginine Residues in Wild-Type CaaD, Free and Complexed with 3-CBA, and Mutants under Various Conditions[a]

	conditions									
	wild type, 3.6 mM sites, pH 7.6, 5 °C, ± 3-CBA				wild type, 1.5 mM sites, pH 6.5, 22 °C		αR8A, 2.8 mM sites, pH 6.5, 22 °C		αR11A, 1.5 mM sites, pH 6.5, 22 °C	
	^{15}Nϵ		NϵH							
arginine resonance	free	complex	free	complex	^{15}Nϵ	NϵH	^{15}Nϵ	NϵH	^{15}Nϵ	NϵH
R_A	86.80	86.80	7.22	7.24	87.62	7.22	87.64	7.20	87.60	7.21
R_B	87.82	87.86	7.34	7.34	88.54	7.33	88.80	7.34	88.80	7.33
R_C	87.76	87.80	7.29	7.30	88.66	7.31	88.42	7.30	89.88	7.32
R_D (αR11)	89.18	89.18	7.11	7.11	89.50	7.12	89.7[b]	7.17[b]		
R_E	89.46	89.46	7.58	7.58	89.62	7.52	89.7[b]	7.51[b]	89.66	7.51
R_F	89.50	89.44	7.24	7.24	89.68	7.23	89.7[b]	7.20[b]	89.78	7.22
R_G (αR8)	89.58	89.68	7.48	7.50	89.94	7.37			90.04	7.37
R_H	89.62	89.62	7.35	7.37			89.8[b]	7.35[b]		
R_I	88.50	88.50	7.22	7.22			88.94	7.28		

[a] The errors in the Nϵ and NϵH chemical shifts are ±0.02 and ±0.01 ppm, respectively. [b] The errors in these Nϵ and NϵH chemical shifts are ±0.1 and ±0.05 ppm, respectively, due to broadened resonances.

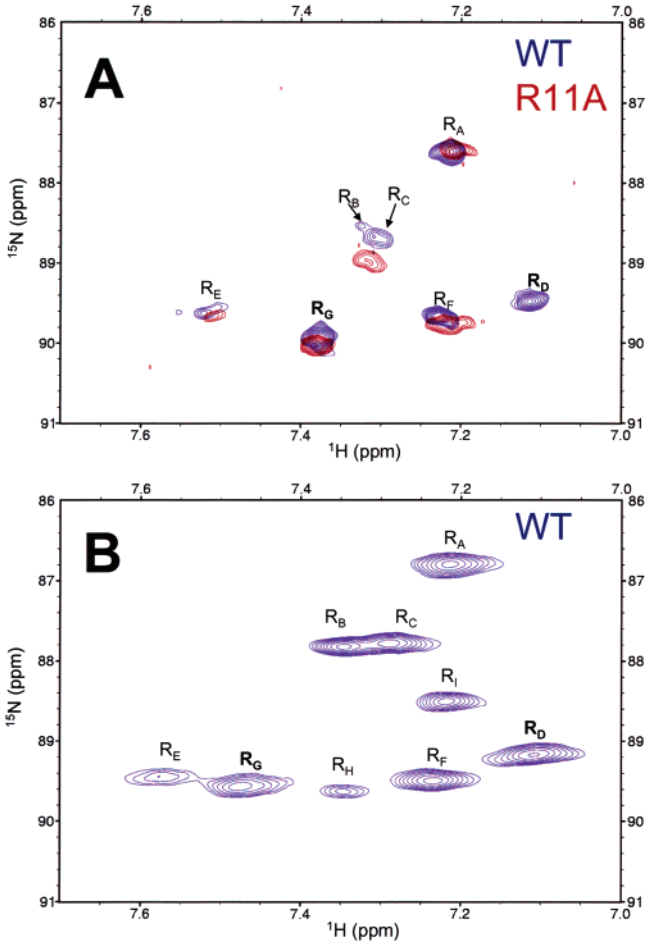

FIGURE 3: ^{1}H−^{15}N spectra of CaaD selective for the Arg-NϵH side chain resonances. The NϵH signals are labeled R_A to R_I and their chemical shifts are given in Table 2. In panel A, the spectra of wild-type CaaD (blue contours) and the αR11A mutant (red contours) are superimposed. Components and conditions were 1.5 mM in CaaD active sites, 8 mM NaH_2PO_4 buffer, pH 6.5, and 10% D_2O, T = 22 °C. Note the disappearance of signal R_D in the spectrum of the αR11A mutant, permitting the assignment of R_D to αArg-11NϵH. Panel B shows the spectrum of wild-type CaaD (3.6 mM in active sites) in 8 mM NaH_2PO_4 buffer, pH 7.6, and 10% D_2O at 5 °C.

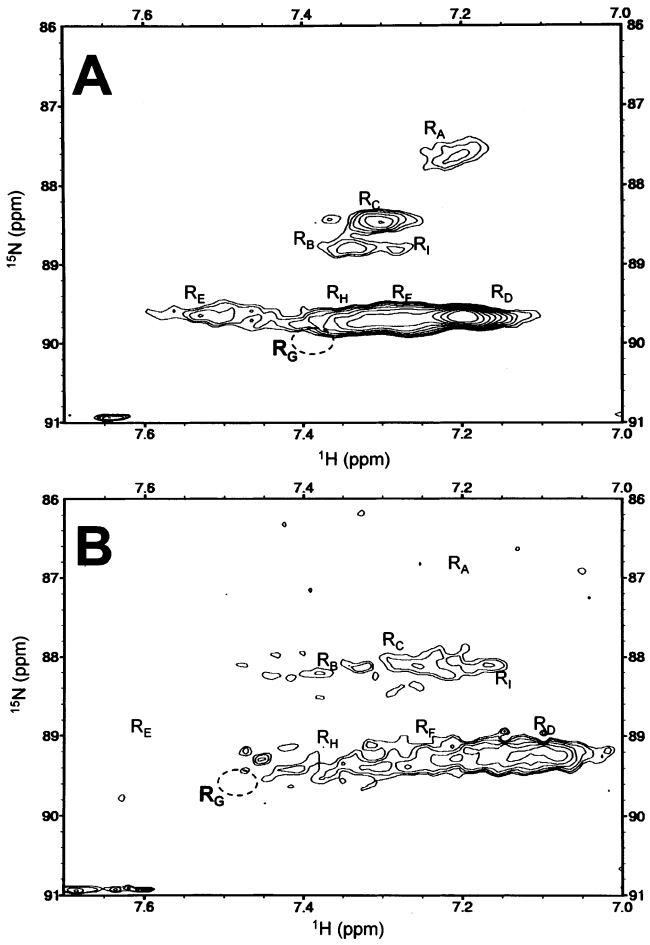

FIGURE 4: ^{1}H−^{15}N spectra of the αR8A mutant of CaaD selective for side chain Arg-NϵH resonances. Panel A shows the spectrum of the αR8A mutant (2.8 mM in active sites) in 8 mM NaH_2PO_4 buffer, pH 6.5, and 10% D_2O at 22 °C. The chemical shifts for the arginine resonances are listed in Table 2. Panel B shows the spectrum of αR8A at pH 7.6 at 5 °C. Conditions are otherwise the same as those in panel A. In panels A and B, the dashed oval indicates the expected position of the missing resonance for R_G on the basis of the spectra shown in Figure 3A,B, obtained under the same conditions. Hence R_G is assigned to αArg-8NϵH.

of βPro-1N, although the last 13−15 residues of the α subunits and the last 13−15 residues of the β subunits are not resolved.

Assignment of the NϵH Resonances of αArg-8 and αArg-11. CaaD has 10 arginine residues, six in the α-subunit (Arg-8, Arg-11, Arg-17, Arg-25, Arg-35, and Arg-43) and four in the β-subunit (Arg-15, Arg-21, Arg-55, and Arg-65) (*1*).

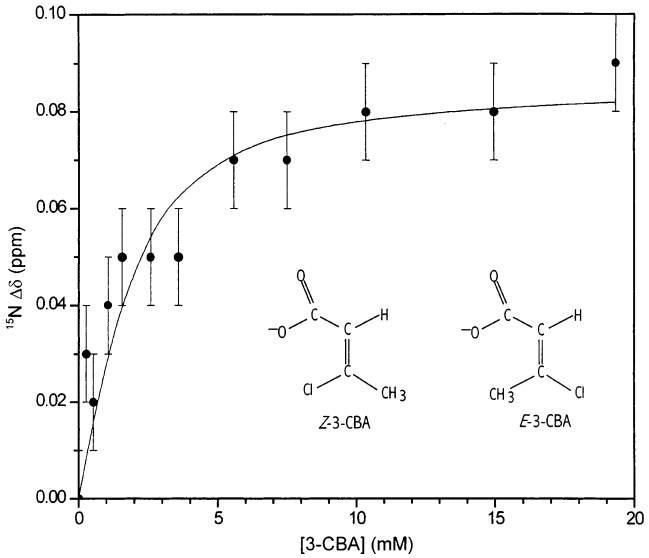

FIGURE 5: Titration of wild-type CaaD with the substrate analogue and competitive inhibitor, 3-CBA, monitoring the Nϵ chemical shift of R_G, assigned to αArg-8. 3-CBA consists of a 6:1 *Z*/*E* isomeric mixture. Components and conditions were 3.6 mM in CaaD active sites in 8 mM NaH_2PO_4 buffer, pH 7.6, and 10% D_2O at 5 °C. The ^{15}N chemical shift changes ($\Delta\delta = \delta_{complex} - \delta_{free}$) were fitted to eq 2 yielding a dissociation constant $K_D = 0.77 \pm 0.44$ mM and a $\Delta\delta_{max}$ of +0.09 ppm.

Scheme 3

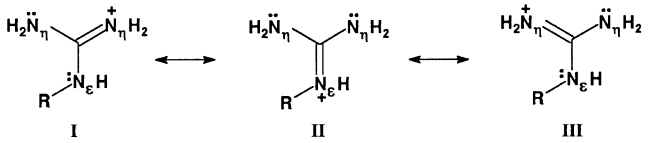

A series of ^{1}H−^{15}N-HSQC spectra selective for the arginine side chains (*8*, *18*) were acquired. The optimal conditions for these experiments are those that minimize the exchange of the NϵH protons, that is, low pH and low temperature. The most important factor was found to be the pH, because at pH values of 6.5 the spectra were well resolved even at 22 °C. Raising the pH above 7.0 required lowering the temperature to 5 °C and increasing the number of transients to obtain good quality spectra. ^{1}H−^{15}N-HSQC spectra of CaaD (1.5 mM in active sites, 22 °C, pH 6.5) showed seven Arg-NϵH resonances (labeled R_A to R_G in Figure 3A, blue contours). At a higher protein concentration (3.6 mM active sites), lower temperature (5 °C), and pH 7.6 and with more transients in the proton dimension (32 instead of 8), nine of the ten Arg-NϵH resonances could be observed (R_A to R_I, Figure 3B) with small chemical shift differences from those in Figure 3A due to the higher pH and lower temperature (Table 2). Under conditions identical to those in Figure 3A, the spectrum of the αR11A mutant (red contours) showed almost exactly the same resonances, except for that of R_D (δH = 7.11 ppm, δN = 89.5 ppm) assigning resonance R_D to αArg-11NϵH.

Such experiments were also performed on two preparations of the αR8A mutant (Figure 4, Table 2). The αR8A samples were less stable than the wild-type enzyme and the αR11A mutant with a strong tendency to precipitate, resulting in broader signals and small changes in some of the arginine NϵH chemical shifts. Nonetheless, at pH 6.5 (Figure 4A), and at pH 7.6 (Figure 4B), there are no well-resolved

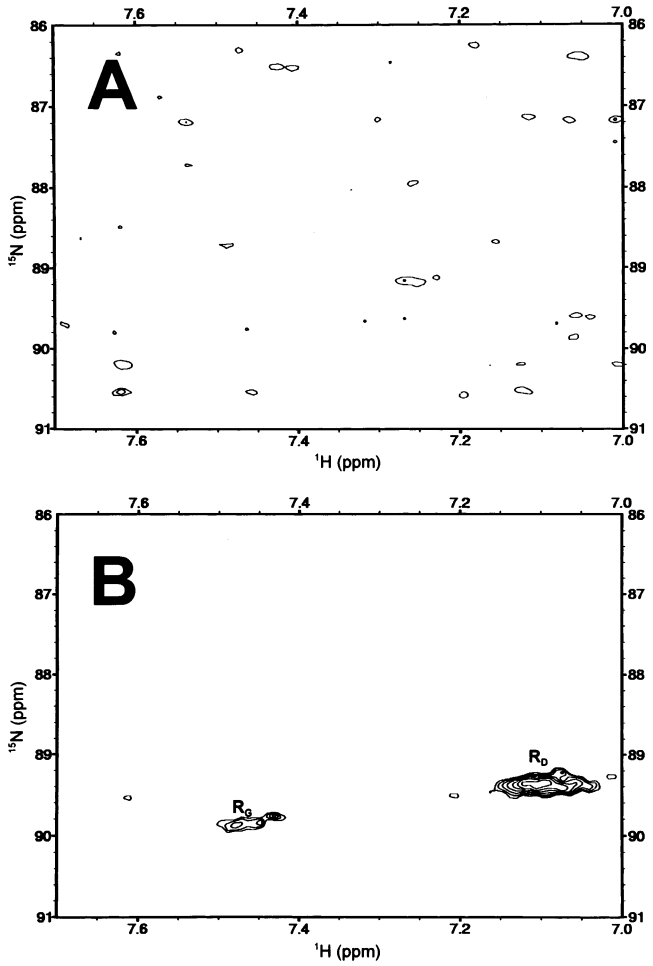

FIGURE 6: Effect of 3-CBA binding on the base-catalyzed NϵH exchange of the arginine residues of CaaD. Panel A shows the ^{1}H−^{15}N spectra at pH 8.9 of wild-type CaaD selective for the side chain Arg-NϵH resonances. Components and conditions were 3.6 mM in CaaD active sites in 8 mM NaH_2PO_4 buffer, pH 8.9, and 10% D_2O at 5 °C. Note, by comparison with Figure 3, the disappearance of all Arg-NϵH resonances. Note also that spectrum A is 40% deeper into the noise level than spectrum B. Panel B was generated with components and conditions the same as those in panel A with the addition of 16 mM 3-CBA (6:1 *Z*/*E*). Note the selective reappearance of R_D and R_G assigned to αArg-11NϵH and αArg-8NϵH, respectively.

resonances near the position of resonance R_G, which was seen with both the wild-type CaaD and the αR11A mutant (Figure 3A,B), suggesting that R_G (δH = 7.37 ppm, δN = 89.8 ppm) is the NϵH signal of αArg-8. These assignments are independently confirmed below.

Selective ^{1}H−^{15}N-HSQC Titrations of Arg-NϵH in Wild-Type CaaD with 3-CBA. The substrate analogue, 3-chlorobutenoic acid, 3-CBA (*Z*/*E* 6:1), was found to be a linear competitive inhibitor of CaaD with a K_I^{slope} of 0.35 ± 0.06 mM, expressed in terms of total 3-CBA concentration, in 20 mM $NaHPO_4$ buffer, pH 9.0, at 25 °C (data not shown). ^{1}H−^{15}N titration of the wild-type enzyme with 3-CBA (*Z*/*E* 6:1) under somewhat different conditions to permit the detection of Arg-NϵH resonances (3.6 mM in active sites, pH 7.6, T = 5 °C) produced no significant changes in chemical shifts, with the exception of the NϵH resonance of αArg-8, which showed progressive downfield ^{15}N shifts (Figure 5). Curve fitting with eq 2 yielded a total chemical shift change of +0.09 ppm in the ^{15}N dimension for αArg-

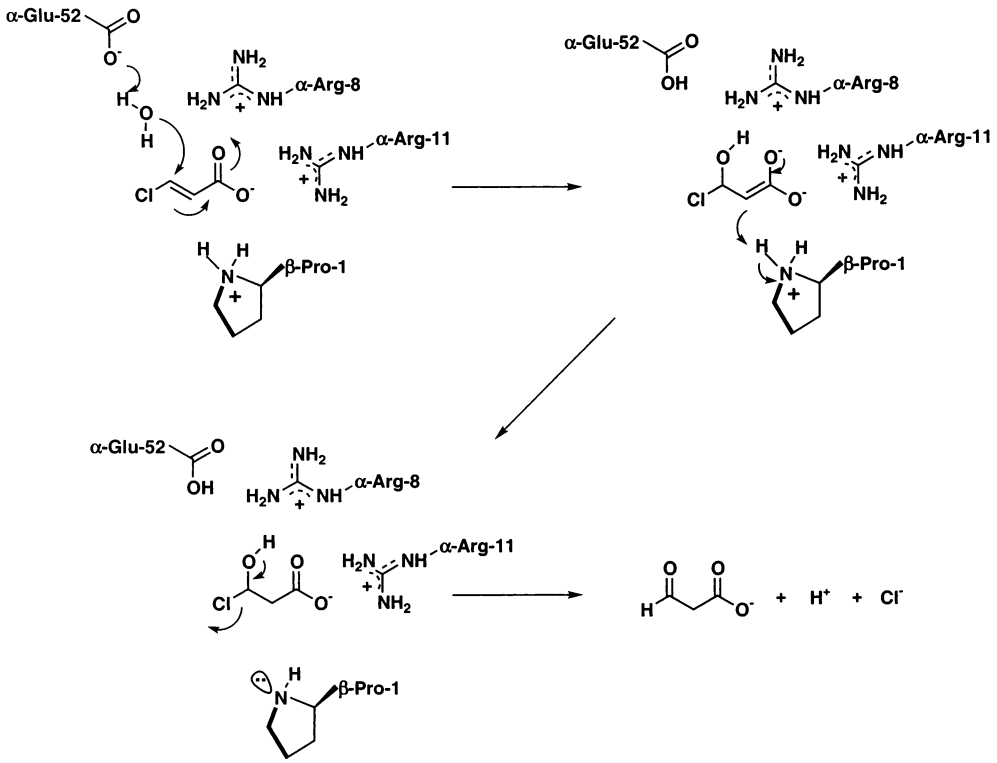

FIGURE 7: Reaction mechanism of CaaD consistent with the results of kinetic, mutagenesis, NMR, and X-ray studies.

8Nϵ and a $K_D = 0.77 \pm 0.44$ mM. This K_D value overlaps with the K_I^{slope} obtained kinetically, consistent with active site binding of 3-CBA (Figure 5). The downfield shift of the αArg-8Nϵ signal in the 3-CBA complex suggests an increased contribution of resonance form II to the structure of αArg-8 (Scheme 3), presumably due to interaction with the anionic ligand. Similar behavior was found in 4-OT where a downfield shift of the Arg-39Nϵ resonance occurred on binding the anionic substrate analogue *cis*,*cis*-muconate (*8*).

Protection against Exchange of Arg-NϵH with Solvent on Binding 3-CBA. Increasing the pH of free CaaD to 8.9 (at 5 °C) resulted in the complete disappearance of all of the nine Arg-NϵH resonances, likely due to accelerated base-catalyzed NϵH exchange (Figure 6A). The addition of a saturating concentration of the substrate analogue, 3-CBA (16 mM) induced the reappearance of only two of the Arg-NϵH signals, R_G and R_D, those assigned by mutagenesis to αArg-8 and αArg-11, respectively (Figure 6B). Hence the active site binding of 3-CBA selectively protects αArg-8 and αArg-11 against base-catalyzed NϵH exchange. This approach represents a novel method for the detection of arginine residues, which function at the active sites of enzymes. The data of Figure 6 are consistent with the presence of two arginine residues at the active site and independently confirm their assignments to αArg-8NϵH and αArg-11NϵH, in agreement with the X-ray data (*4*). The kinetic, mutagenesis, and NMR studies thus support roles for both αArg-8 and αArg-11 in binding the substrate, and possible intermediates, in the reaction mechanism of CaaD.

The Catalytic Mechanism of CaaD. Figure 7 provides a reasonable mechanism for CaaD consistent with the available data, although other mechanisms cannot be ruled out. In this mechanism, αGlu-52 deprotonates a water molecule which, in a Michael addition, adds to C3 of the substrate to form a carbanion ↔ aci-carboxylate intermediate, stabilized by both αArg-8 and αArg-11. The interaction of two cationic arginine residues with one carboxylate is consistent with a dianionic aci-carboxylate intermediate. In the next step, *β*Pro-1 protonates C2 to complete the addition of water. The halo-alcohol intermediate then loses the C-3-OH proton and eliminates the halide ion to form the malonate semialdehyde product. Alternative mechanisms might involve either the concerted addition of water across the C-2, C-3 double bond of the substrate, or the prior protonation at C-2 to form a carbocation intermediate. While the concerted addition cannot be dismissed, a carbocation intermediate is likely to be destabilized by the two arginine residues in the active site, making it the least attractive mechanism.

A comparison of k_{cat} of the CaaD reaction (3.8 s^{-1}, Table 1) with the pseudo-first-order rate constant for the uncatalyzed addition of water to fumarate, extrapolated to room temperature and to pH 9.0 ($10^{-13.6}$ s^{-1}) (*24*), indicates a rate acceleration by CaaD of $10^{14.2}$-fold. A very similar rate acceleration of $10^{13.9}$-fold is obtained by comparing k_{cat} of CaaD with the pseudo-first-order rate constant of the hydroxide-catalyzed dehalogenation of CAA, extrapolated to room temperature and to pH 9.0 ($10^{-13.3}$ s^{-1}) (*25*). From the data of Table 1, *β*Pro-1, αGlu-52, αArg-8, and αArg-11 each contribute factors of $\geq 10^{3.4}$ to k_{cat}. If the effects of these four residues are additive, their total contribution to k_{cat} is $> 10^{13.6}$, which is comparable to the catalytic power of this enzyme. Hence the mechanism of Figure 7 may provide both a qualitative and quantitative explanation of catalysis by CaaD.

CONCLUSIONS

CaaD likely represents a recently evolved activity within the tautomerase superfamily and provides evidence for the catalytic and structural versatility of the *β*-α-*β* structural fold.

Further elucidation of the principles used in nature to vary the reactivities of key catalytic components in this simple β-α-β structural motif may assist in understanding how new biocatalysts evolve using this basic scaffolding. The results of this study demonstrate versatility in the catalytic roles of Pro-1 within the 4-OT family: it can be utilized as either a general base, as in 4-OT (*6*, *7*), or a general acid, as in CaaD. In the case of CaaD the role of βPro-1 as a general acid catalyst is demonstrated by its pK_a of 9.2 ± 0.2 obtained by pH titrations measuring both catalytic activity and the ^{15}N chemical shift of this residue. Having thus identified the general acid, the role of general base catalyst might reasonably be assigned to αGlu-52, the only residue with the required characteristics among those known to be essential for the activity of the enzyme (Table 1).

The other two residues essential for the activity of CaaD, αArg-8 and αArg-11, were studied by selective ^{1}H−^{15}N-HSQC NMR measurements, which detected nine of the ten Arg-NϵH signals. Selective Arg-HSQC spectra of the αR11A and αR8A mutants were used to assign their respective NϵH signals. The K_D value of the substrate analogue 3-CBA obtained by NMR titration, monitoring the ^{15}N chemical shift of αArg-8Nϵ, agreed within error with the kinetically determined K_I^{slope} of 3-CBA suggesting that αArg-8 interacted with this substrate analogue at the active site. Two of the nine detectable ArgNϵH resonances in the wild-type enzyme, those of αArg-8 and αArg-11, were shown to be selectively protected against base-catalyzed NϵH exchange at pH 8.9 by binding the substrate analogue 3-CBA, supporting their participation in substrate binding. A mechanism of CaaD (Figure 7) showing the catalytic roles of βPro-1, αGlu-52, αArg-8, and αArg-11, consistent with the results of kinetic, mutagenesis, NMR, and X-ray studies, may provide both a qualitative and quantitative explanation of catalysis by this enzyme.

ACKNOWLEDGMENT

We thank Dr. William H. Johnson, Jr., for synthesizing 3-chloro-2-butenoic acid.

REFERENCES

1. Poelarends, G. J., Saunier, R., and Janssen, D. B. (2001) *trans*-3-Chloroacrylic acid dehalogenase from *Pseudomonas pavonaceae* 170 shares structural and mechanistic similarities with 4-oxalocrotonate tautomerase, *J. Bacteriol. 183*, 4269−4277.
2. Poelarends, G. J., Kulakov, L. A., Larkin, M. J., van Hylckama Vlieg, J. E. T., and Janssen, D. B. (2000) Roles of horizontal gene transfer and gene integration in evolution of 1,3-dichloropropene- and 1,2-dibromoethane-degradative pathways, *J. Bacteriol. 182*, 2191−2199.
3. Poelarends, G. J., Wilkens, M., Larkin, M. J., van Elsas, J. D., and Janssen, D. B. (1998) Degradation of 1,3-dichloropropene by *Pseudomonas cichorii* 170, *Appl. Environ. Microbiol. 64*, 2931−2936.
4. de Jong, R. M., Brugman, W., Poelarends, G. J., Whitman, C. P., and Dijkstra, B. W. (2004) The X-ray structure of *trans*-3-chloroacrylic acid dehalogenase reveals a novel hydration mechanism in the tautomerase family, *J. Biol. Chem. 279*, in press.
5. Azurmendi, H. F., Wang, S. C., Massiah, M. A., Whitman, C. P., and Mildvan, A. S. (2003) New role for the amino-terminal proline in the tautomerase superfamily: *trans*-3-chloroacrylic acid dehalogenase, *Biochemistry 42*, 8619, Abstracts of 226th ACS National Meeting, Sept. 11−17, 2003, New York, NY. Abs. No. BIOL 113.
6. Stivers, J. T., Abeygunawardana, C., Mildvan, A. S., Hajipour, G., and Whitman, C. P. (1996) Catalytic role of the amino-terminal proline in 4-oxalocrotonate tautomerase: affinity labeling and heteronuclear NMR studies, *Biochemistry 35*, 803−813.
7. Stivers, J. T., Abeygunawardana, C., Mildvan, A. S., Hajipour, G., and Whitman, C. P. (1996) 4-Oxalocrotonate tautomerase: pH dependence of catalysis and pK_a values of active site residues, *Biochemistry 35*, 814−823.
8. Harris, T. K., Czerwinski, R. M., Johnson, W. H., Jr., Legler, P. M., Abeygunawardana, C., Massiah, M. A., Stivers, J. T., Whitman, C. P., and Mildvan, A. S. (1999) Kinetic, stereochemical, and structural effects of mutations of the active site arginine residues in 4-oxalocrotonate tautomerase, *Biochemistry 38*, 12343−12357.
9. Wang, S. C, Person, M. D., Johnson, W. H., Jr., and Whitman, C. P. (2003) Reactions of *trans*-3-chloroacrylate dehalogenase with acetylene substrates: consequences of and evidence for a hydration mechanism, *Biochemistry 42*, 8762−8773.
10. Sambrook, J., Fritsch, E. F., and Maniatis, T. (1989) *Molecular Cloning: A Laboratory Manual*, Cold Spring Harbor Laboratory, Cold Spring Harbor, NY.
11. Laemmli, U. K. (1970) Cleavage of structural proteins during the assembly of the head of bacteriophage T4, *Nature 227*, 680−685.
12. Waddell, W. J. (1956) A simple ultraviolet spectrophotometric method for the determination of protein, *J. Lab. Clin. Med. 48*, 311−314.
13. Ho, S. N., Hunt, H. D., Horton, R. M., Pullen, J. K., and Pease, L. R. (1989) Site-directed mutagenesis by overlap extension using the polymerase chain reaction, *Gene 77*, 51−59.
14. Mayer, K. L., and Stone, M. J. (2000) NMR solution structure and receptor peptide binding of the CC chemokine eotaxin-2, *Biochemistry 39*, 8382−8395.
15. Neidhardt, F. C., Bloch, P. L., and Smith, D. F. (1974) Culture medium for enterobacteria, *J. Bacteriol. 119*, 736−747.
16. Weber, D. J., Abeygunawardana, C., Bessman, M. J., and Mildvan, A. S. (1993) Secondary structure of the MutT enzyme as determined by NMR, *Biochemistry 32*, 13081−13088.
17. Delaglio, F., Grzesiek, S., Vuister, G. W., Zhu, G., Pfeifer, J., and Bax, A. (1995). NMRPipe: a multidimensional spectral processing system based on UNIX pipes, *J. Biomol. NMR 6*, 277−293.
18. Zhang, O., Kay, L. E., Olivier, P. J., and Forman-Kay, J. D. (1994) Backbone ^{1}H and ^{15}N resonance assignments of the N-terminal SH-3 domain of drk in folded and unfolded states using enhanced-sensitivity pulsed field gradient NMR techniques, *J. Biomol. NMR 4*, 845−858.
19. Segel, I. H. (1975) *Enzyme Kinetics*, pp 888−898, John Wiley & Sons, Inc., New York.
20. Czerwinski, R. M., Harris, T. K., Massiah, M. A., Mildvan, A. S., and Whitman, C. P. (2001) The structural basis for the perturbed pK_a of the catalytic base in 4-oxalocrotonate tautomerase: kinetic and structural effects of mutations of Phe-50, *Biochemistry 40*, 1984−1995.
21. Subramanya, H. S., Roper, D. I., Dauter, Z., Dodson, E. J., Davies, G. J., Wilson, K. S., and Wigley, D. B. (1996) Enzymatic ketonization of 2-hydroxymuconate: specificity and mechanism investigated by the crystal structures of two isomerases, *Biochemistry 35*, 792−802.
22. Taylor, A. B., Czerwinski, R. M., Johnson, W. H., Jr., Whitman, C. P., and Hackert, M. L. (1998) Crystal structure of 4-oxalocrotonate tautomerase inactivated by 2-oxo-3-pentynoate at 2.4 Å resolution: analysis and implications for the mechanism of inactivation and catalysis, *Biochemistry 37*, 14692−14700.
23. Stivers, J. T., Abeygunawardana, C., Whitman, C. P., and Mildvan, A. S. (1996) 4-Oxalocrotonate tautomerase, a 41-kDa homohexamer: backbone and side-chain resonance assignments, solution secondary structure, and location of active site residues by heteronuclear NMR spectroscopy, *Protein Sci. 5*, 729−741.
24. Wolfenden, R., and Snider, M. J. (2001) The depth of chemical time and the power of enzymes as catalysts, *Acc. Chem. Res. 34*, 938−945.
25. Braddon, S. A., and Dence, C. N. (1968) Structure and reactivity of chlorolignin, I. alkaline hydrolysis of chlorine-substituted lignin model compounds, *Tappi 51*, 249−256.

BI030241U